Fabrication of high-quality joints between Gd–Ba–Cu–O bulk superconductors

N Tutt[1],* , **J Congreve[1]** , **Y Shi[1]** , **D Namburi[1,2]** , **A Dennis[1]** , **H Druiff[1] and J Durrell[1]**

[1] Department of Engineering, University of Cambridge, Cambridge, United Kingdom
[2] Electronic and Nanoscale Engineering, University of Glasgow, Glasgow, United Kingdom

E-mail: nialltutt1998@gmail.com

CrossMark

Abstract

This work reports a technique for fabricating superconducting joints between GdBCO-Ag bulk superconductors, using YBCO-Ag as an intermediate joining material. The ability to provide reliable joints between multiple bulk superconductors overcomes many of the challenges of fabricating large superconductors or machining hard and brittle bulk superconductors into practical shapes. We report on nine single grains of GdBCO-Ag which have been joined with a YBCO-Ag intermediate. Samples were cut and joined in a variety of c-plane orientations to refine and understand the effect this had on the superconducting properties of jointed samples. The trapped field of pre-jointed and jointed bulk superconductors were compared; the maximum trapped field achieved was 59% of the pre-jointed sample. Further analysis showed that the critical temperature and critical current of the samples were degraded by the jointing process. Microstructural and chemical analysis showed that the jointing process facilitated diffusion of silver towards the joint and in some cases large pores were formed at the joint interface. These factors consequently inhibited current flow across the joint and thus reduced the maximum trapped field achievable when compared to the original unjointed sample.

Keywords: bulk superconductors, superconductor jointing, superconductor welding, GdBCO-Ag joining, superconductor joining

(Some figures may appear in colour only in the online journal)

1. Introduction

There are a wide range of potential applications for bulk superconductors. These span compact magnetic resonance imaging (MRI) machines, Maglev trains, energy storage flywheels and high efficiency motors and generators. There are, however, many challenges associated with the fabrication, industrial scale-up, and post-processing of large bulk superconductors.

Material brittleness makes machining difficult, hence complex geometries cannot be easily fabricated [1–5].

Given the significant technological potential of these materials, there has been considerable focus upon the fabrication of single-grained (RE)–Ba–Cu–O [(RE)BaCuO] bulk superconductors, where (RE) is a rare earth element such as yttrium (Y) or gadolinium (Gd). These materials are of particular interest because of their high critical temperature (T_c), current density (J_c) and magnetic trapped field. To avoid the deleterious effects of grain boundaries, a large single-grain must be fabricated, this is achieved through a peritectic decomposition reaction of $(RE)Ba_2Cu_3O_7$ (RE-123) and an excess of $(RE)_2BaCuO_5$ (RE-211) and a subsequent seeded re-crystallisation. The larger the single-grained region within a bulk superconductor, the greater the size of the current loop

which can flow uninterrupted within it and thus a greater magnetic field can be achieved. The trapped magnetic fields (RE)BCO bulk superconductors can achieve are significantly larger than those achieved by conventional magnets [1, 6–9]. Growth of samples larger than 30 mm in diameter has, however, generally led to a deterioration of superconducting properties as well as reduced mechanical strength and inhomogeneous penetration of oxygen during post-growth oxygenation [5, 10].

To overcome the challenges surrounding growth, machining and complex geometries; small bulk superconductors may be joined to form a larger composite grain. This would provide a larger area over which the superconducting current can flow and thus enable a larger magnetic field to be trapped. In order to achieve this, there must be low crystallographic misorientation angles between the individual grains and good connectivity between the joined pieces.

There are a number of factors used to determine the quality of a superconducting joint [3]:

(1) Values of J_c across the joint and consequent trapped magnetic field- these should be comparable in magnitude to those of the original individual pieces.
(2) The trapped magnetic field profile- this should exhibit the characteristics of a single grain, which is typically a singular peak in the trapped field profile.
(3) The mechanical strength of the joint-this must be sufficiently high to withstand Lorentz forces as well as vibrations, acoustic noise and other mechanical stresses experienced during operation.

Techniques used to form joints between bulk superconductors can be grouped into four categories. These are solid-state diffusion, infiltration joining, welding using an intermediate material with a lower peritectic temperature and joining using a non-superconducting intermediary to locally lower the peritectic temperature of the interface between the (RE)BCO bulks [11–21].

The solid-state diffusion method does not use an intermediate material to form the joint, instead it relies upon heating the pieces of bulk superconductor, without melting, so that they fuse together. For this process to be effective, the two interfaces of the joint must be highly polished to provide the greatest effective contact area. Initial attempts to achieve high critical current values across the joint were poor. These values were an order of magnitude lower than achieved in the original samples [11, 15].

Infiltration joining is similar to the infiltration growth process [22, 23]. RE-211 powder is compacted between the pieces of bulk superconductor and a liquid source powder is placed above this. Several heating profiles have been trialled and good crystallographic alignment with homogenous RE-211 inclusions, low porosity and few mechanical defects have been reported. In all cases, despite the formation of strong mechanical joints and a promising microstructure, superconducting property data has not been reported [12, 13].

Techniques relying on localised reduction of the peritectic temperature utilised a thin layer of silver as an intermediate material. The metallic intermediary lowered the peritectic temperature of the (RE)BCO at the joint interface. A variety of thicknesses of silver were trialled at a range of temperatures. The (RE)BCO material in close proximity to the silver intermediate reached the peritectic temperature sooner and then recrystalised during the cooling process. This process was shown to form robust mechanical joints while maintaining high values of J_c across the joint [16].

The welding process entails using an intermediate piece of (RE)BCO as a thin layer between two larger (RE)BCO pieces to form a superconducting joint. Research has primarily focussed upon welding YBCO due to its relatively low peritectic temperature compared to other (RE)BCO systems. Early attempts used a Y-211, Y-123, PtO_2 mix in the form of a sintered bulk intermediate to join two YBCO bulk pieces using a peritectic decomposition reaction. This was shown to form a strong mechanical joint which had good superconducting properties when compared with the sintered bulk superconductors available at the time [17].

Thulium (Tm) based intermediate materials have also been investigated as a method to weld YBCO bulks. The superconducting properties were not comparable with the original YBCO sample, likely due to crystal orientation mismatch and impurities from the TmBCO and YBCO moving towards the weld during heating [18, 19]. Similarly, ErBCO solder has been used as a welding material with a YBCO bulk and has indicated strong magnetic coupling between the two materials; this research also highlights the relationship between sound mechanical joints, the lack of residual liquid phase in the joining region and strong crystal alignment facilitating high current flow across the joint [20, 21, 24].

Unlike previous work, which has focussed on joining YBCO, this work reports on the joining of GdBCO-Ag bulk superconductors which have a higher peritectic temperature than YBCO. Joints have been fabricated using a thin single-grained slice of YBCO-Ag intermediate material. The YBCO-Ag intermediate has a lower peritectic temperature than the surrounding GdBCO-Ag and therefore will melt in preference to the GdBCO-Ag bulk superconductor. Greater consideration must be given to the migration of silver during the joining process as previous joining attempts have used silver-free YBCO as the bulk material. The welding of GdBCO-Ag samples is of particular industrial interest, as GdBCO-Ag samples are simpler to fabricate compared to YBCO, are more widely available from commercial suppliers and have more desirable superconducting and mechanical properties.

In this paper, we present a simple and rapid route to fabricate joints between GdBCO-Ag bulk superconductors. These joints are mechanically robust and exhibit promising superconducting properties, achieving up to 59% of the maximum trapped field of the original samples. The degradation in superconducting properties has been explained through measurements of critical temperature, critical current and observations of the microstructure.

2. Methodology

2.1. Sample growth

Nine samples of GdBCO-Ag were fabricated by top seed melt growth (TSMG) using precursor powder consisting of 46 g of Gd-123:Gd-211:CeO_2:Ag_2O of 99.9% purity in the mass ratio 150:50:1:20. This was pressed uniaxially in a 25 mm diameter cylindrical die. A buffer pellet of 5 mm in diameter was pressed from 0.2 g of precursor powder of composition Gd-123:Gd-211:CeO_2 in the mass ratio 150:50:1 and was placed at the centre of the top surface. A generic seed was then placed on top of the buffer pellet [24].

Three YBCO-Ag samples were fabricated by liquid-phase-assisted TSMG to provide the intermediate joining material [25]. The main pellet was uniaxially pressed from a layer of 4.6 g of liquid phase consisting of Yb_2O_3:$Ba_3Cu_5O_8$:BaO_2 of 99.9% purity in the mass ratio 5.0:5.6:1.0 (previously calcined at 1123 K for 5 h) below a layer of 46 g of Y-123:Y-211:CeO_2:Ag_2O in the mass ratio 150:50:1:20 in a 25 mm diameter cylindrical die. A buffer pellet of 5 mm in diameter was pressed from 0.2 g of precursor powder of composition Y-123:Y-211:CeO_2 in the mass ratio 150:50:1 was placed at the centre of the top surface. A Mg-doped NdBCO generic seed crystal was then placed on top of the buffer pellet.

Each precursor arrangement was then placed on three Yb_2O_3 coated, yttria-stabilised ZrO_2 rods. The coating has a lower peritectic temperature than that of the YBCO precursor powder and hence reduces the likelihood of secondary nucleation occurring at the base of the compact.

After the growth process, the sample was heated in an oxygen-rich environment for 10 d at 723 K to transform the Gd-123 from a non-superconducting tetragonal matrix to a superconducting orthorhombic crystal structure.

2.2. Trapped field measurement

The samples were field cooled to 77 K with an applied magnetic field of 1.4 T. The trapped field was measured before and after jointing.

After magnetisation, the maximum trapped field was measured using a single hand-held Hall probe positioned 0.5 mm above the sample surface. The trapped field profile for the top and base of the samples were then measured using a rotating array of 19 Hall probes positioned approximately 2 mm from the sample surface.

2.3. Joining process

Six of the GdBCO-Ag samples were sliced in half and three were sliced into quarters using a rotating saw equipped with a diamond particle impregnated wheel. The jointing faces of each sample were then progressively polished using silicon carbide paper from 120 to 4000 grit. The orientations of the cuts in relation to the facet lines are shown figure 1.

YBCO-Ag samples were sliced in sections approximately 2–3 mm in depth. These were then polished as previously described, to provide smooth contact with the GdBCO-Ag bulk pieces.

Samples were secured using a top loading method, whereby two pieces of machinable ceramic with V-shaped grooves enabled the sample to be firmly wedged into position. Table 1 below provides details on the cut direction and c-axis orientation of each sample during joining.

Firm contact between all pieces is required to produce a strong mechanical joint; the mechanical integrity of the joint typically correlates with the ability of the superconducting current to flow between the joined sections.

Figure 2 shows the clamping arrangements for a sample cut in half, a 0.1 kg load is applied uniaxially to the two segments of GdBCO-Ag to ensure firm contact with the YBCO-Ag intermediate material.

A heating profile was established which ensured the peritectic temperature of the larger GdBCO-Ag pieces of 1293 K (1020 °C) was not exceeded. Initial rapid heating at 500 K h^{-1} to a temperature of 1223 K followed by a hold of 1.5 h allowed the system to reach a sufficient temperature to create a joint between all three pieces.

A schematic of the heating profile is shown in figure 3.

After the jointing process was completed, the sample was heated once again in an oxygen-rich environment for 10 d at 723 K.

It should be noted that samples B1, B2, B3 and B4 as well as D1 and D2 are direct repeats used to investigate the repeatability of the results.

2.4. J_c and T_c measurement

Both before and after joining, sample A1 was cut in half along a diameter to expose a rectangular cross section and then cut further into sub-specimens of approximate dimensions $\sim$1 mm $\times$ 2 mm $\times$ 2 mm, as shown in figure 4. These sub-specimens were analysed using a SQUID (superconducting magnetic interference device) magnetometer (Quantum Design MPMS 3). The value of T_c was established directly from the measured data at a constant field of 1.6 kA m^{-1} ($\sim$20 G) and the value of J_c at 77 K was derived from the observed hysteresis loop using the extended Bean critical state model [26].

2.5. Microstructure and composition

Jointed sample A1 was cut perpendicular to the slice of YBCO-Ag joining intermediate to expose a rectangular cross-section. This was then progressively polished. The microstructure of the sample was observed using a scanning electron microscope (SEM) at 2000$\times$ magnification using an acceleration voltage of 25 kV across an area of approximately 700 μm $\times$ 700 μm at intervals of 1 mm. Images were taken at the locations shown in figure 5. Images were taken at a distance 1 mm away from the edge of the YBCO-Ag joining material. The distribution of RE-211, silver and pores were observed. The average composition for each area approximately 700 μm $\times$ 700 μm imaged using the SEM was analysed
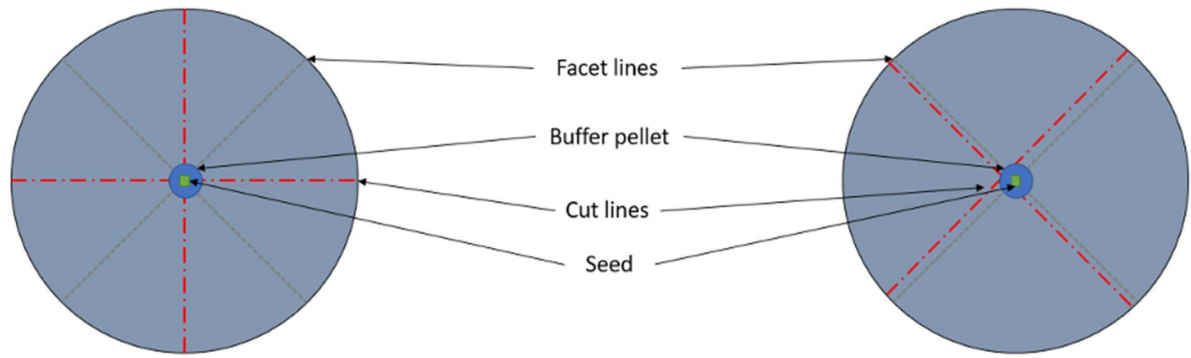
Figure 1. Cutting and jointing orientations for GdBCO-Ag samples. Cutting direction bisecting the facet line (left) and along the facet line (right).

Table 1. Sample cut and joining orientation, the white arrows in the diagrams indicate the relative orientation of the c-axis of each segment.

Sample	Cut direction	c-plane orientation	c-plane orientation
A1	In half along facet line	Two segments in opposing orientation	
B1 B2 B3 B4	In half along facet line	All segments in the same orientation	
C1	In half bisecting facet lines	All segments in the same orientation	
D1 D2	In quarters along facet line	All segments in the same orientation	
E1	In quarters bisecting facet lines	Two segments in opposing orientation	
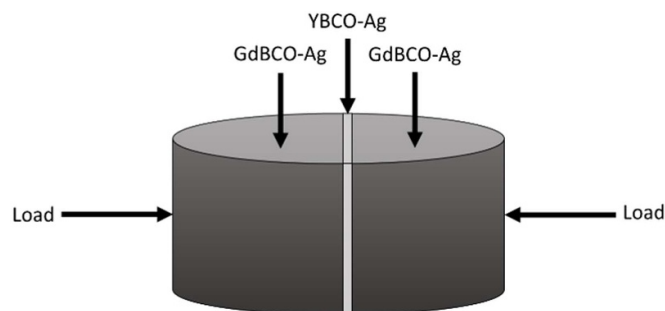
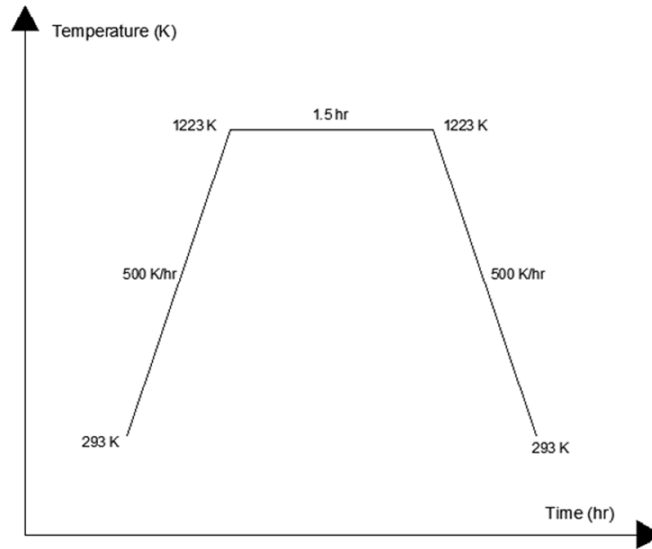**Figure 2.** The assembly for joining GdBCO-Ag with a YBCO-Ag intermediate.

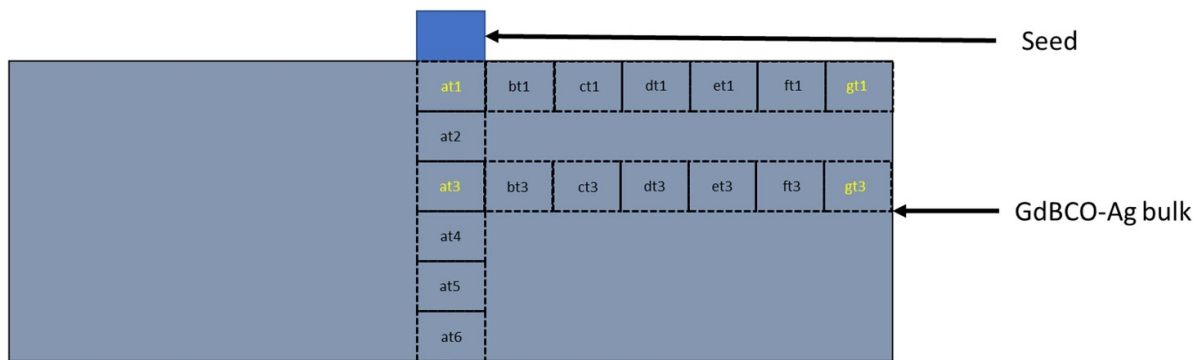**Figure 3.** Heating profile used to join GdBCO-Ag with a YBCO-Ag intermediate.

Figure 4. Locations of the sub-specimens used for SQUID analysis; the sub-specimens highlighted in yellow were measured.
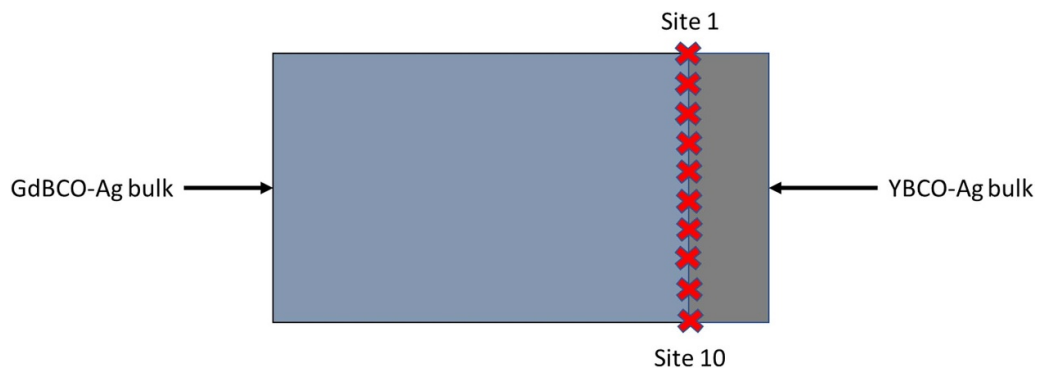

Figure 5. Location of sites from where the images were captured employing a scanning electron microscope.

using energy dispersive x-ray spectrometry (EDX). The composition data was normalised according to the atomic percentages of Y, Ba, Cu and Ag present at each location.

3. Results and discussion

3.1. Electromagnetic characteristics

The GdBCO-Ag samples were cut and joined in a variety of orientations to assess the impact that joint orientation has on current flow across the joint. Samples were also joined in different relative *c*-axis orientations to further understand how this may impact current flow and consequently the maximum trapped field.

In all cases, a strong mechanical joint was formed which could withstand manual handling as well as its own weight.

Photographs of two of the joined samples are shown in figure 6 below, this shows sample B1—cut and then joined along the facet line and sample C1—cut bisecting the facet line and joined.

The maximum trapped field at both the bottom and top of the original and joined samples can be seen below in table 2.

Sample A1 was cut along the facet line and then joined with the two segments in opposing *c*-axis orientation to provide a potential worst-case scenario. Due to the crystallographic mismatch between the two segments, current flow between the three pieces is limited and thus the maximum achievable trapped field is reduced. This is shown by the comparably low maximum trapped field of 29% of the original sample.

Additional samples which were cut in half and jointed with their *c*-axes oriented in the same direction, generally exhibited a higher maximum trapped field percentage post-jointing. Sample B1 displayed a maximum trapped field of 30%. The magnetic field profile showed two distinct peaks when both the top and bottom of the sample were measured, highlighting that a superconducting joint is unlikely to have been formed.

Sample B2 did however exhibit a trapped field profile with a single peak at the top surface. Concentric circles on the trapped field plot indicated unabated current flow across the bulk and joining material and thus a superconducting joint.

The joined sample which displayed the best superconducting properties was sample B3 where a trapped field of 59% of the original was achieved. Not only did this show the highest trapped field measurements of any sample but also the most promising trapped field profile. At both the top and the bottom surfaces, the trapped field profile of the joined sample exhibited an uninterrupted set of concentric flux lines with no secondary peaks, as can be seen in figure 7, demonstrating good superconducting properties.

Sample B3 used the same orientation and cut direction as samples B1, B2 and B4, however each of these jointed samples achieved a different percentage of the maximum trapped field of the original sample. These differences can be attributed to a number of factors. The hand polishing of the materials in the joining process means that each join is not perfectly
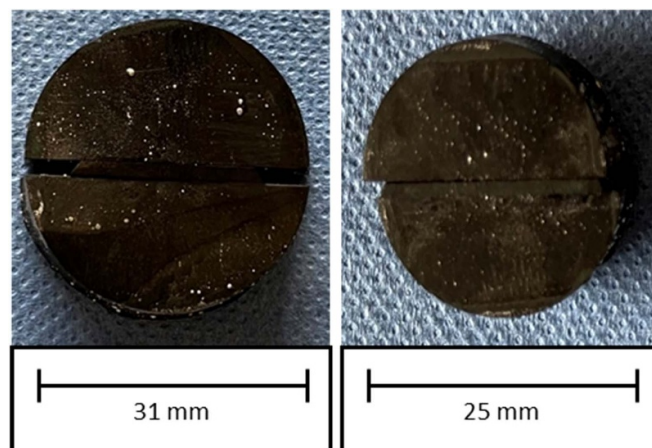

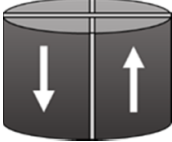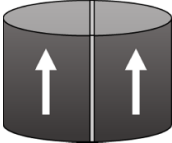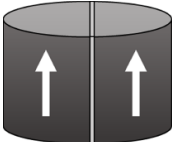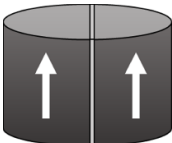**Figure 6.** Sample B1 (left) and sample C1 (right) after joining.
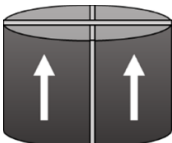
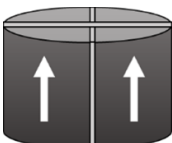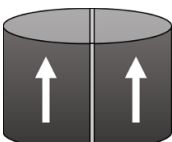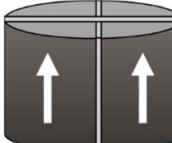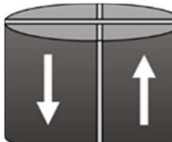repeatable; the clamping arrangement is not flawless and some movement of the materials in the furnace during the jointing heating cycle may lead to differences in the quality of the joints. Microscopic factors, such as the differences in diffusion of silver during jointing and the distribution of pores at the joint interfaces within each of the joined samples, may lead to further differences in the trapped field profile.

In order to establish that joints between two halves of the samples were superconducting and that the trapped field profiles were not simply two separate peaks, sample B4 was cut and the two halves placed in a steel container to hold them in place. These were then magnetised, and the trapped field profile measured. The sample was later joined to allow a comparison. Figure 8 shows the trapped field profiles of the unjointed halves (left) and the jointed sample (right) of sample B4. Whilst both the unjointed and jointed samples show two peaks, the jointed sample has a clear dominant peak with concentric flux lines supporting it, as opposed to the unjointed sample where concentric flux lines clearly outline the two individual pieces in their entirety. The joint however showed low trapped field values post-joining at only 18% of the original.

Sample C1 appears to have formed a superconducting joint at the top surface, which has been reflected in the trapped field measurement post-jointing of 37% of the original. The magnetic field at the bottom of the joined sample, has two distinct peaks however and does not appear to be superconducting. This demonstrates the difference in the quality of joints along the *c*-axis of a sample and the effects potential inhomogeneities can have on current flow across a joint. Furthermore, the quality of the joint is affected by the alignment of the individual pieces within the system, ensuring good alignment is complicated and therefore it is difficult to ensure the entire interface of the GdBCO-Ag bulk pieces and the YBCO-Ag joining material are in contact.

Comparison of samples C1 and B1–4 demonstrates the limited effect of cut direction upon the quality of the joint. Samples C1 and B1–4 were all joined in the same *c*-axis orientation however sample C1 was cut bisecting the sample

Table 2. Maximum trapped field data measured at 77 K using the handheld hall probe for the original and joined samples.

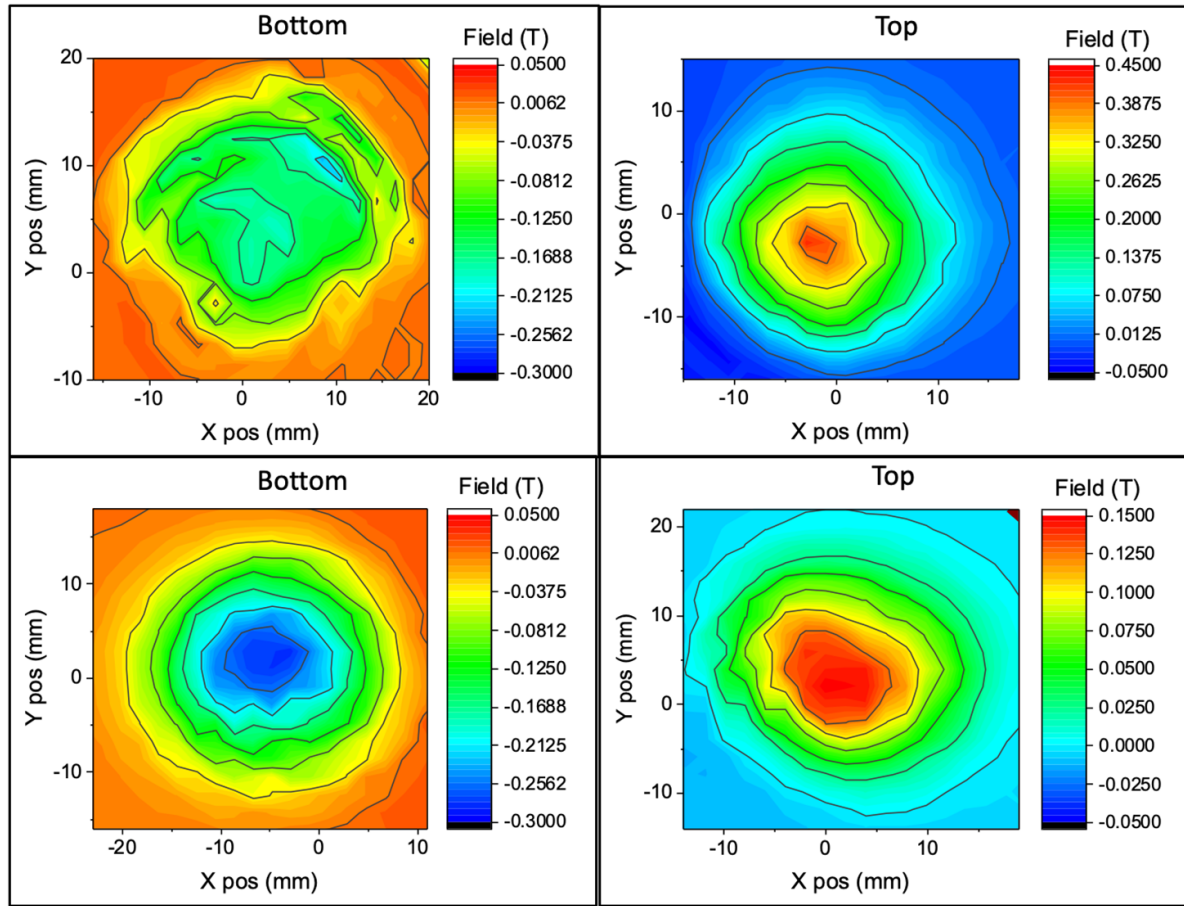| Sample	Original samples		Joined samples		Average percentage of original (%)	c-plane orientation diagram
	Max B_t on the top (T)	Max B_t on the bottom (T)	Max B_t on the top (T)	Max B_t on the bottom (T)		
A1	0.56	0.41	0.12	0.16	29	
B1	0.80	0.56	0.25	0.17	30	
B2	0.48	0.42	0.20	0.21	44	
B3	0.63	0.38	0.40	0.21	59	
B4	0.88	0.69	0.17	0.13	18	
C1	0.46	0.30	0.17	0.12	37	
D1	0.62	0.41	0.18	0.13	30	
D2	0.88	0.60	0.28	0.29	38	
E1	0.73	0.40	0.17	0.11	24	

Figure 7. Trapped field profiles at 77 K for sample B3 pre-jointing (top quadrants) and post-jointing (bottom quadrants).
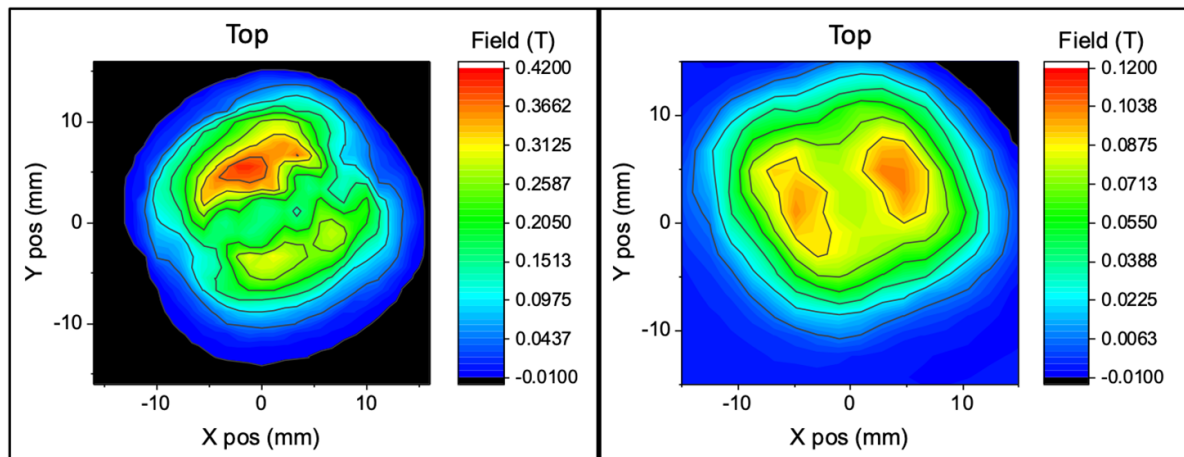

Figure 8. Trapped field profiles at 77 K for sample B4 unjointed (left) and jointed (right).

facet lines, all samples had comparable maximum trapped field results.

In addition to joining halves of samples, attempts were made to join samples cut into quarters. It was anticipated that there would be a significant reduction in the maximum trapped field achieved due to the number of joints required. A reduction in maximum trapped field after joining comparable to the samples which were cut in half was seen in both samples and D1 and E1. The maximum trapped field reduction was therefore not as severe as may have been predicted, with sample D1 achieving a post-joining trapped field measurement 30% of the original maximum trapped field.

Sample D2 was joined using the same process, cut direction and *c*-axis orientation as sample D1, however shows a slight improvement in the percentage of maximum trapped field retained post-jointing at 38%. This characteristic may be
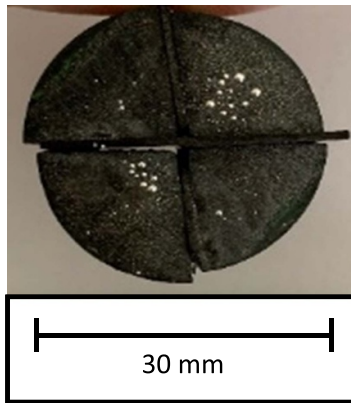
Figure 9. Sample E1-note the air gap between two of the joined segments.

attributed to small variations in the joining process (including polishing and clamping arrangements) and inhomogeneities in the crystallographic structure. Both samples D1 and D2 have results comparable to those samples cut in half and joined in the same *c*-axis orientation. The number of joints within the same bulk is therefore not thought to significantly reduce the current flow.

Sample E1 was joined using the same procedure however a misalignment error during clamping led to an air gap between two pieces, as shown in figure 9.

Sample E1 provides additional evidence the joints are superconducting. The airgap prevents the flow of superconducting current across this region of the joint. This is shown by the shape of the flux contours and is marked in the bottom left image of figure 10 by a black circle. Although the joint was only partially successful and achieved a relatively low maximum trapped field, the air gap between two quarters demonstrated the profile of a non-superconducting joint and showed clearly that there was some current flow across the remainder of the joint area. If the three remaining joints were not at all superconducting, they would show similar inclusions to the air gap in the contour lines. Therefore, at least partial superconductivity of the joints appears to have been achieved.

In summary, the macroscopic evidence of the GdBCO-Ag jointing process demonstrates that a highly effective superconducting joint can be formed. The orientation of the cut is not thought to have a significant impact on the ability of current to flow unabated across the joint nor is the number of joints within the sample. However, the relative *c*-plane orientation of joining was shown to have a major impact, as shown by lower proportional trapped field measurements in samples A1 and E1. This is due to the crystallographic mismatch between the top and bottom of the sample, poorer crystallographic structure at the bottom of samples and reduced homogeneity at the bottom of samples.

Most joined samples achieved a maximum trapped field ~30%–40% of the original magnitude, with further improvements possible through improving the reliability of the joint fabrication process. This improved joining process with consistent predictability would allow designers to utilise joined

GdBCO-Ag bulk superconductors for applications where magnetic flux is required over a larger area.

3.2. Critical temperature and critical current analysis

Values of T_c and J_c were measured for the four sub-specimens from sample A1 both before and after joining, sub-specimen locations are shown in figure 4. The joining process reduced the critical temperature at the two central sub-specimens *at1* and *at3*; by 1.45 K 4.77 K respectively. There were negligible increases at sites *gt1* and *gt3* which can be attributed to small variations in the location of sub-specimens analysed for the pre- and post-jointed sample; at the edge of the sample there is a greater variation in quality. Table 3 shows the value T_c for each sub-specimen.

The transition width between the superconducting and non-superconducting state was calculated, ΔT. Sub-specimens *at1* and *at3* showed a reduction in ΔT of 1.75 K and 1.69 K respectively, although a decrease in ΔT at central sample sites may be seen as advantageous, this was primarily attributed to the reduction of absolute critical temperature in these sub-specimens. Sites *gt1* and *gt3* were shown to have considerably higher ΔT post-joining indicating a clear degradation in quality. Data for the transition width for each sub-specimen can be seen in table 3.

Generally, the critical current was shown to decrease post-joining and may be attributed to the diffusion of silver and a less homogeneous structure following additional heating during joint fabrication. In particular sample at 3 was shown to decrease significantly from 19 025 A cm^{-2} to 958 Acm^{-2} this may be attributed to the diffusion of silver into the jointing region and that the jointed sample may contain some YBCO-Ag which generally has a lower $J_c(0)$ than GdBCO-Ag. The exception to this trend is *at1* which saw an increase in $J_c(0)$ from 7094 Acm^{-2}–11 665 Acm^{-2}, this may be caused by a slight difference in the location of the sub-specimen between the joined and unjointed samples. Table 3 shows the difference in $J_c(0)$ for each sub-specimen.

3.3. Microstructure

The SEM images of sample A1, shown in figure 11 shows that the quality of the join varies greatly throughout the sample. Image 2, taken approximately 4 mm from the top of the *c*-axis, shows that silver has diffused into this air gap. Although silver is electrically conductive, the presence of silver at the interface will inhibit the flow of supercurrent at the joint.

In the centre of the sample at image 3 (in figure 11), a continuously joined region has formed with expected strong superconducting properties. The YBCO-Ag section of the sample has a high concentration of silver. However, there are limited pores at the interface between the GdBCO-Ag bulk and the intermediate joining material. Hence in this region, there will be high current flow and a good quality mechanical joint.

Image 4 (of figure 11) indicates a continuously joined region, similar to that of image 3, however a large pore is present in the GdBCO-Ag. Similar to the properties exhibited
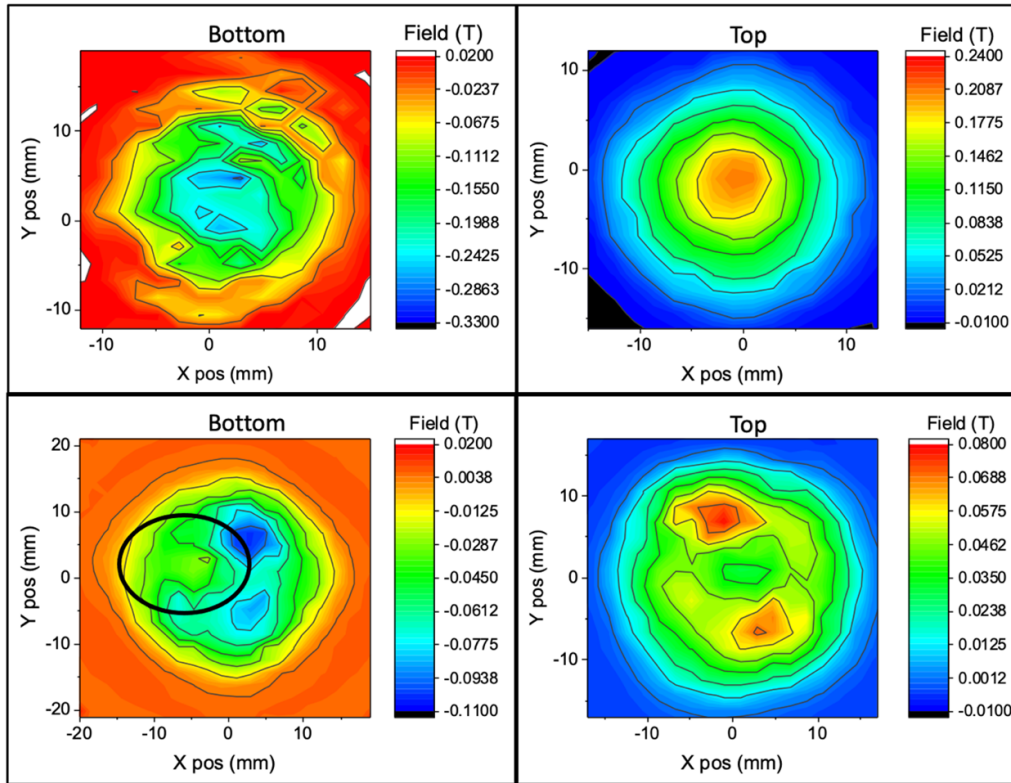
Figure 10. Trapped field profiles at 77 K for sample E1 original (upper quadrants) and jointed (lower quadrants). The area indicated in the bottom left of the image corresponds to the region due to the air-gap, as described in the text.

Table 3. Summary of critical temperature, critical temperature transition and critical current for sub-specimens at1, at3, gt1 and gt3.

		Sub-specimen			
Measurement	Sample	at1	at3	gt1	gt3
Critical temperature (K)	Original sample	92.66	93.09	92.51	91.89
	Jointed sample	91.21	88.32	92.52	92.03
Critical temperature transition (K)	Original sample	5.01	1.93	1.91	6.03
	Jointed sample	3.26	0.24	8.74	9.70
Critical current (A cm^{-2})	Original sample	7094	19 025	7182	10 875
	Jointed sample	11 665	958	4861	5175

in image 1, zero current will flow across the pore and the mechanical quality of the joint will have been partially degraded in this region.

Image 6 (of figure 11) shows a large air gap between the two materials and will have a similar effect on both the mechanical and superconducting properties to that described in image 1.

3.4. Composition analysis

Composition analysis of sample A1 using energy dispersive x-ray spectroscopy (EDX) has shown that there has been diffusion of Y into the Gd bulk and that Gd has diffused across the joint into the Y joining material. This diffusion of Y and Gd particles indicates good connectivity between

the pieces. This diffusion may be responsible for lowering the T_c of the sub-specimens at the joint interface after joining (sub-specimens *at1* and *at3*) and the reason negligible change is observed in the values of T_c in the *gt* sub-specimens pre- and post-joining. The lack of Y within the *gt* sub-specimens, does not account for the change in temperature transition sharpness, ΔT, therefore subsequent heating can be said to degrade the overall quality of the bulk superconductor.

The diffusion of Y and Gd occurred up to a distance of approximately 1 mm into both samples. This is likely to be caused by the peritectic reaction close to the interface between the two materials. Figure 12 shows the respective distributions of Gd and Y in the system at site 4, as shown in figure 5 (approximately 4 mm from the top of the sample) with an
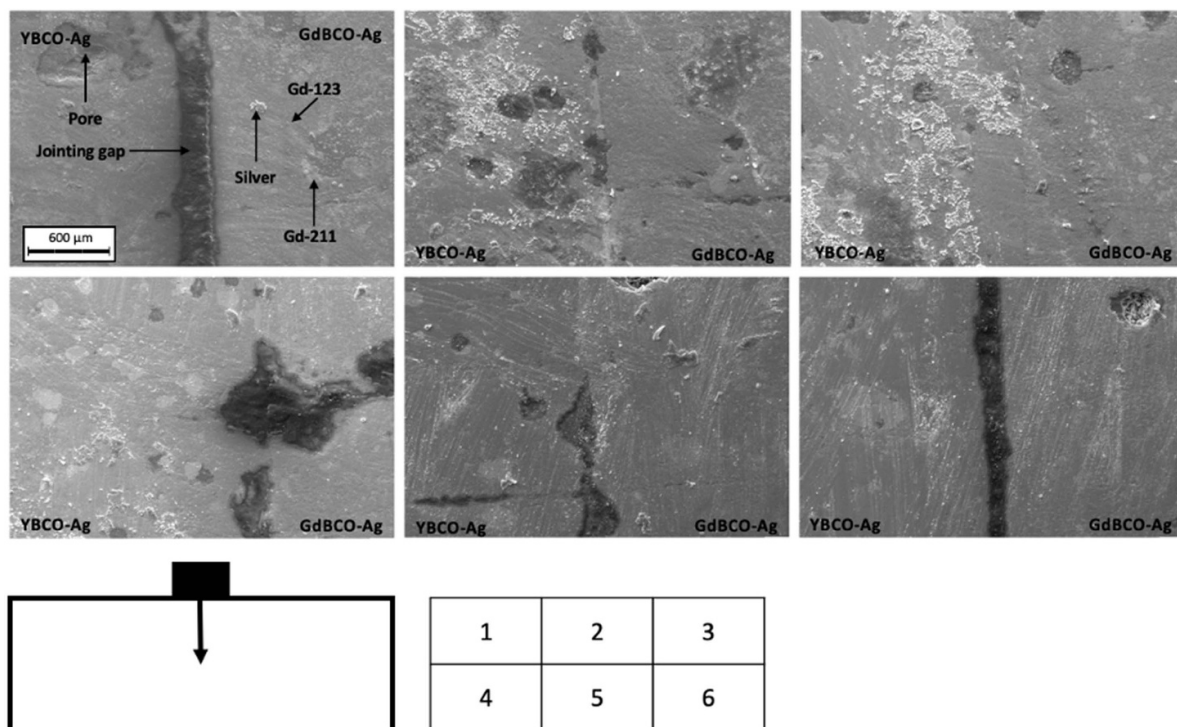
Figure 11. SEM images of sample A1 in the c-plane. Top left image is the top of the sample and bottom right image is the bottom of the sample. Image position decreases (L–R) by approximately 2 mm and pictures were taken in the order indicated on the key (1–6). YBCO-Ag material is to the left of the jointing gap and GdBCO-Ag material is to the right of the jointing gap in each image.
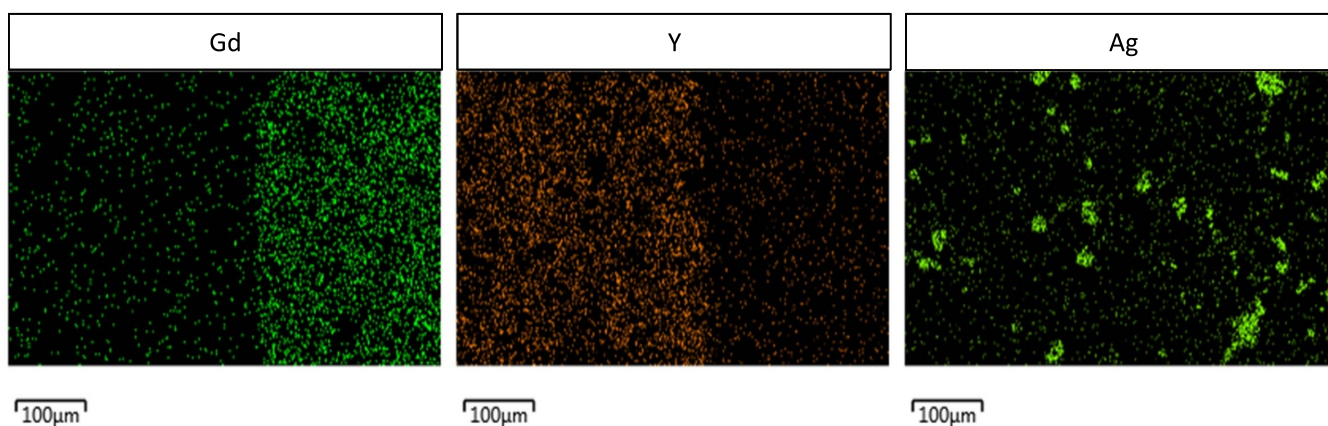

Figure 12. Elemental maps taken at site 4. Gd, Y and Ag distributions are shown from left to right.

even distribution of silver in both the bulk and the joining material.

4. Conclusion

A reliable technique to join single-grained GdBCO-Ag bulk superconductors using a YBCO-Ag intermediate has been developed. These joints are mechanically robust and display promising superconducting properties. The higher peritectic temperature and inclusion of silver within the GdBCO-Ag system provides additional challenges as compared to joining

within the YBCO systems, hence the joint fabrication is more complex.

The relative *c*-axis orientation of the joined pieces was shown to have a major impact on the trapped field characteristics post-joining while the direction of the cut relative to the facet line was shown to have limited impact.

Composition analysis has shown inter-diffusion of gadolinium and yttrium at the joint interface. Thissuggests that at these locations there is good contact between the interfaces and so there must be good physical connectivity between these regions, however this diffusion may cause a reduction in the localised critical temperature and critical current. Microscopic

analysis has also shown visible diffusion of silver into the joining region which may inhibit current flow and limit the superconducting properties of the system.

Further refinement of this process will allow manufacturers to fabricate large, intricately shaped GdBCO-Ag grains from small, high-quality single grains. This simple joint fabrication technique described, twinned with promising superconducting properties provides numerous opportunities for the practical application of bulk superconductors. GdBCO-Ag bulks are of particular industrial interest due to their comparably simple fabrication process, widespread commercial availability and desirable superconducting and mechanical properties.

Data availability statement

The data that support the findings of this study are openly available at the following URL/DOI: https://doi.org/10.17863/CAM.91146.

Acknowledgments

ORCID iDs

N Tutt ⬥ https://orcid.org/0000-0001-7828-382X
J Congreve ⬥ https://orcid.org/0000-0002-2025-2155
Y Shi ⬥ https://orcid.org/0000-0003-4240-5543
J Durrell ⬥ https://orcid.org/0000-0003-0712-3102

References

[1] Durrell J H *et al* 2014 A trapped field of 17.6 T in melt-processed, bulk Gd-Ba-Cu-O reinforced with shrink-fit steel *Supercond. Sci. Technol.* **27** 082001
[2] Campbell A M and Cardwell D A 1997 Bulk high temperature superconductors for magnet applications *Cryogenics* **37** 567–75
[3] Congreve J V J, Dennis A R, Shi Y, Bumby C W, Druiff H, Cardwell D A and Durrell J H 2021 A reliable technique to fabricate superconducting joints between single grain, Y-Ba-Cu-O bulk superconductors *Supercond. Sci. Technol.* **34** 094003
[4] Congreve J V J, Shi Y, Huang K Y, Dennis A R, Durrell J H and Cardwell D A 2019 Improving mechanical strength of YBCO bulk superconductors by addition of Ag *IEEE Trans. Appl. Supercond.* **29** 1–5
[5] Durrell J H, Ainslie M D, Zhou D, Vanderbemden P, Bradshaw T, Speller S, Filipenko M and Cardwell D A 2018 Bulk superconductors: a roadmap to applications *Supercond. Sci. Technol.* **31** 103501
[6] Shiohara Y and Endo A 1997 Crystal growth of bulk high-Tc superconducting oxide materials *Mater. Sci. Eng.* R **19** 1–86
[7] Nariki S, Sakai N, Murakami M and Hirabayashi I 2004 High critical current density in RE-Ba-Cu-O bulk superconductors with very fine RE_2BaCuO_5 particles *Physica* C **412** 557–65
[8] Babu N H, Iida K and Cardwell D A 2006 Enhanced magnetic flux pinning in nano-composite Y-Ba-Cu-O superconductors *Physica* C **445** 353–6
[9] Murakami M, Yamaguchi K, Fujimoto H, Nakamura N, Taguchi T, Koshizuka N and Tanaka S 1992 Flux pinning by nonsuperconducting inclusions in melt-processes YBaCuO superconductors *Cryogenics* **32** 930–5
[10] Shi Y, Dennis A R, Zhou D, Namburi D K, Huang K, Durrell J H and Cardwell D A 2016 Factors affecting the growth of multiseeded superconducting single grains *Cryst. Growth Des.* **16** 5110–7
[11] Bradley A D, Lo W, Mironova M, Babu N H, Cardwell D A, Campbell A M and Salama K 2001 Microstructure and growth of joins in melt-textured $YBa_2Cu_3O_{7-\delta}$ *J. Mater. Res.* **16** 2298–305
[12] Schmitz G J, Tigges A and Schmidt J C 1998 Microstructural aspects of joining superconductive components using solder *Supercond. Sci. Technol.* **11** 73–75
[13] Manton S J, Beduz C and Yang Y 1999 Rejoining of single grain melt textured bulk $YBa_2Cu_3O_{7-x}$ *IEEE Trans. Appl. Supercond.* **9** 2089–92
[14] Iliescu S, Granados X, Puig T and Obradors X 2006 Growth mechanism of Ag-foil-based artificially superconducting joints of $YBa_2Cu_3O_7$ monoliths *J. Mater. Res.* **21** 2534–41
[15] Cardwell D A, Bradley A D, Babu N H, Kambara M and Lo W 2002 Processing, microstructure and characterization of artificial joins in top seeded melt grown Y–Ba–Cu–O *Supercond. Sci. Technol.* **15** 639–47
[16] Iliescu S, Granados X, Bartolomé E, Sena S, Carrilllo A E, Puig T, Obradors X and Evetts J E 2004 High critical current $YBa_2Cu_3O_7$ artificial joints using Ag foils as welding agent *Supercond. Sci. Technol.* **17** 182–5
[17] Shi D 1995 Formation of a strongly coupled $YBa_2Cu_3O_x$ domain by the melt-joining method *Appl. Phys. Lett.* **66** 2573–5
[18] Zheng H, Jiang M, Nikolova R, Welp U, Paulikas A P, Huang Y, Crabtree G W, Veal B W and Claus H 1999 High critical current "weld" joints in textured $YBa_2Cu_3O_x$ *Physica* C **322** 1–8
[19] Prikhna T A *et al* 2002 Superconducting joining of melt-textured YBCO *Physica* C **372–6** 1528–30
[20] Iida K, Yoshioka J, Negichi T, Noto K, Sakai N and Murakami M 2002 Strong coupled joint for Y–Ba–Cu–O superconductors using a sintered Er–Ba–Cu–O solder *Physica* C **378–81** 622–6
[21] Yoshioka J, Iida K, Negichi T, Sakai N, Noto K and Murakami M 2002 Joining Y123 bulk superconductors using Yb-Ba-Cu-O and Er-Ba-Cu-O solders *Supercond. Sci. Technol.* **15** 712–6
[22] Namburi D K, Shi Y, Dennis A R, Durrell J H and Cardwell D A 2018 A robust seeding technique for the growth of single grain (RE) BCO and (RE) BCO-Ag bulk superconductors *Supercond. Sci. Technol.* **31** 044003
[23] Namburi D K, Shi Y, Palmer K G, Dennis A R, Durrell J H and Cardwell D A 2016 A novel, two-step top seeded infiltration and growth process for the fabrication of single

grain, bulk (RE)BCO superconductors *Supercond. Sci. Technol.* **29** 095010

[24] Shi Y, Babu N H and Cardwell D A 2005 Development of a generic seed crystal for the fabrication of large grain (RE)-Ba-Cu-O bulk superconductors *Supercond. Sci. Technol.* **18** L13–6

[25] Congreve J V J, Shi Y, Dennis A R, Durrell J H and Cardwell D A 2018 The successful incorporation of Ag into single grain, Y–Ba–Cu–O bulk superconductors *Supercond. Sci. Technol.* **31** 035008

[26] Bean C P 1962 Magnetisation of hard superconductors *Phys. Rev. Lett.* **8** 250–3